A Systematic Classification and Typological Assessment Method for Mortise and Tenon Joints

Bin Shang,[a] Zhe Chen,[b,]* Yuxi Lin,[a] Hong Chang,[c] and Jianing Wei [b]

* Corresponding author: czsdjtu@outlook.com

DOI: 10.15376/biores.19.3.4918-4940

GRAPHICAL ABSTRACT

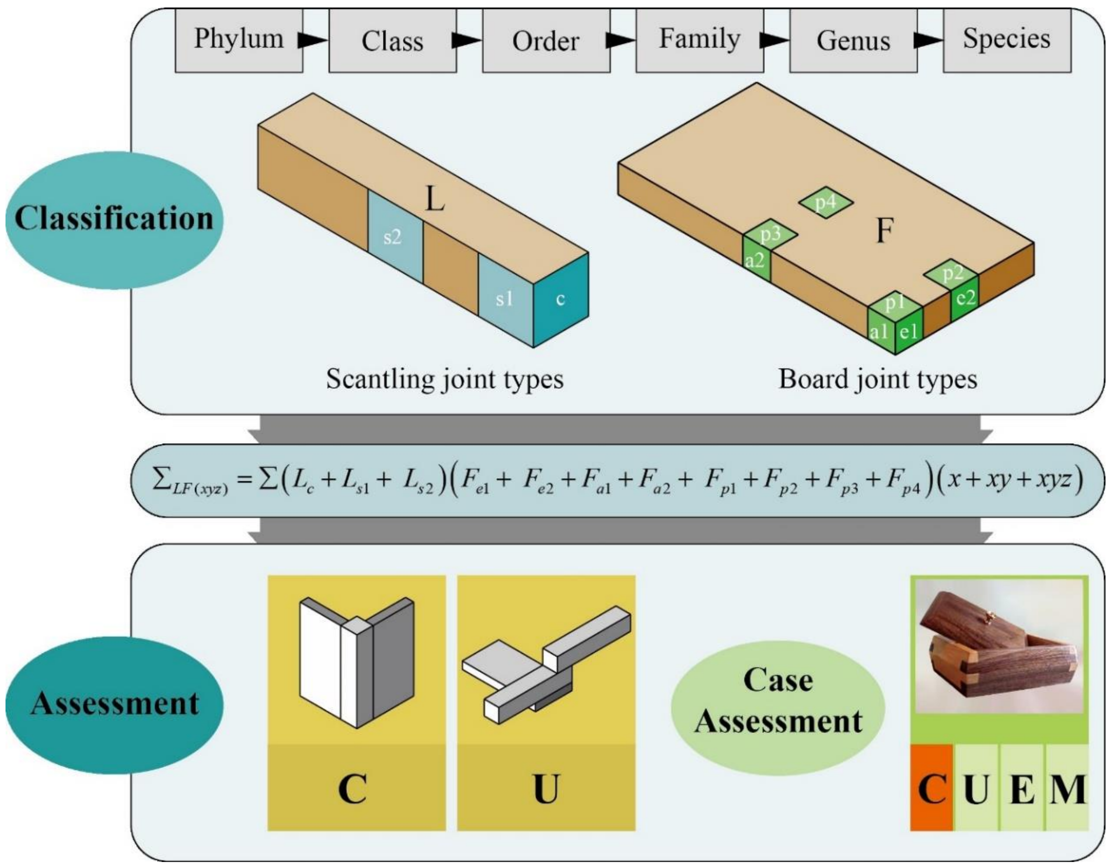

A Systematic Classification and Typological Assessment Method for Mortise and Tenon Joints

Bin Shang,[a] Zhe Chen,[b,]* Yuxi Lin,[a] Hong Chang,[c] and Jianing Wei [b]

The classification of Mortise and Tenon (MT) joints is vital, as it enables standardized terminology, facilitates comparative analysis, and enhances understanding of construction techniques across a variety of applications including the design, manufacturing, and management of wood products. Although the classification of MT joints is crucial, current research in this area lacks a systematic approach. The study adopts a morphological composition paradigm to investigate MT joints. This study introduces a 6-level classification index hierarchy for MT morphology, employing methods from biological classification and arithmetic cross-method coding. By encoding joint features and morphological composition, the study delineates 352 possible joint types and 1056 theoretical compositions across dimensions, elucidating diverse structural logics and aiding comprehension. Next, a feasibility typicality assessment identifies 198 typical and 310 atypical morphological types, presented clearly in graphical form. Validations are conducted through analysis of 2654 research cases, which are encoded according to the index hierarchy, thereby affirming the scientific validity and practical utility of the classification system.

DOI: 10.15376/biores.19.3.4918-4940

Keywords: Mortise and Tenon joint; Structure classification; Typicality assessment

Contact information: a: School of Architecture and Design, China University of Mining and Technology, Xuzhou, 221116, China; b: Shandong Jiaotong University, Jinan, 250357, China; c: School of Mechanics and Civil Engineering, China University of Mining and Technology, Xuzhou, 221116, China;
** Corresponding author: czsdjtu@outlook.com*

INTRODUCTION

Timber is a sustainable and renewable resource that is widely applied across the construction and furniture sectors (Švajlenka and Kozlovská 2020). The Mortise and Tenon (MT) joint is a traditional connection for wood structures, relying on the natural interlocking mechanism enhanced by the cyclic forces generated by the components themselves. This design allows for controlled flexibility in the parts, which in turn bolsters the structural integrity by enhancing energy absorption and resistance to bending (Xie *et al*. 2021). The semi-rigid nature of these joints contributes to the longevity and durability of wooden structures (Feio *et al*. 2014). As their structural efficacy and sustainability, MT joints are pervasively incorporated into various wooden products such as furniture, bridges, toys, handicrafts, vehicles, sports equipment, *etc*. (Shang *et al*. 2023).

The origins of MT construction technology can be traced back to the perforation techniques of the Paleolithic era. The shouldered stone axes that used perforation nesting and binding to join stone tools and wooden sticks are considered the earliest form of MT (Li 2015). Research on MT joints has a long history (Ma *et al*. 2020). With the long-term exploration of the construction characteristics and physical properties of wood by humans, the structural principles and construction methods of MT have gradually been clarified (Hassan *et al*. 2023). Currently, academic research on MT has distinct disciplinary characteristics. Mechanical strength and structure are the primary research focuses for MT joints, with aesthetics gaining increasing attention in recent years (Yang and Wang 2013; Elek *et al*. 2020; Hu and Liu 2020; Qiao *et al*. 2022). Under the "Dual-Carbon" background, sustainable design methods such as reduction principle in the green design concept are focused on the MT joints (Bragança *et al*. 2010; Wu *et al*. 2021b). Additionally, studies on the MT joint have been extended to other fields, such as the realm of composite materials, MT joint selection and prefabricated frame tunnels model (Huang *et al*. 2023; Li *et al*. 2023; Yilmaz and Burdurlu 2023; Darwesh *et al*. 2024).

Although various studies have been conducted on MT joints, there are still some limitations. Most research on MT structural styles tends to focus on characteristic experiments of existing MT forms or case innovation research. Moreover, the morphological classification of MT joints presents varying perspectives among researchers of diverse cultural backgrounds and regions, owing to the abundance and diversity of case sources. Existing approaches to classification are characterized by excessive granularity and data overload, rendering exhaustive analysis impractical and comprehensive research challenging. Consequently, significant divergence exists in research conclusions within this domain. To date, no universally recognized classification method or indexing system for MT forms has been established. However, considering the fundamental characteristics of wood and structural mechanics, all MT joints exhibit inherent regularities in material utilization and core principles in form design, governed by consistent principles of change. To fill this gap, this article adopts a novel research approach, examining the logic of MT joints and proposing a classification indexing method based on morphological construction paradigms.

Utilizing morphological feature induction, biological classification methodologies, and linear pairing algorithms, this study systematically codes the relationship between MT joint forms and component features, constructing a rigorous, comprehensive, and foundational standardized indexing system. Through visual analysis, nearly 200 typical MT structural forms are categorized at the 'genus level'. The findings of this research offer a scientific and convenient naming and indexing framework for the development and application of MT structural styles, with the potential to unveil new research directions and application scenarios in the field. Also, the systematic classification of MT joints streamlines wood product design, manufacturing, and management, inspiring innovation, enhancing efficiency, and driving field advancement.

Research on MT Joints

In morphological studies, studies have delved into the analysis and classification of MT joints based on their forms and historical origins (Guan 2007; Chen 2014; Tsai *et al.* 2022). By categorizing the different types of MT joints, researchers aim to uncover the principles that have allowed these structures to persist throughout history and across cultures. The restoration, strengthening, and innovative applications of traditional MT joints represent another pivotal area of study. Experts including Eckelman and Smardzewski have significantly contributed to the analysis of wood product structures, including experimental and numerical studies on the effects of internal assembly forces and selected materials on stiffness and bending moments, as well as comparative studies and optimization of various mortise-and-tenon structures (Eckelman and Haviarova 2011; Smardzewski 2015; Uysal *et al.* 2015; Kasal *et al.* 2016; Taghiyari *et al.* 2018).

Some studies have also explored the merits and shortcomings of these joints, proposing solutions for their repair and reinforcement when damaged (Li *et al*. 2015; Wu *et al*. 2021a). Moreover, there is an interest in how traditional MT forms can be adapted or innovated for contemporary woodworking practices (Feio *et al*. 2014; Liu and Lin 2020; He *et al*. 2021). The morphology and scale of typical MT joints have also been subjects of scrutiny. These studies focus on the modification and transformation of MT forms to better suit specific industrial applications, emphasizing the need for design flexibility and innovation to meet the demands of various domains (Ohmori and Kunii 2011; Claus and Seim 2020; Hu and Chen 2021). The aesthetic and decorative functions of MT joints have not been overlooked in the academic discourse. Others have investigated the aesthetic appeal of these structures, considering their role in enhancing the visual appeal of woodwork, emphasizing the dual nature of MT joints as both functional elements and artistic expressions (Wu and Geng 2015; Sun 2021). The study of the physical properties of MT joints has been a focal point for researchers. Other studies also have delved into the structural mechanics and material properties of these joints, assessing their performance in terms of withdrawal state, bending load, shear strength, seismic strength, and service life under various conditions (Branco and Descamps 2015; Demirci *et al*. 2020; Pan *et al*. 2024).

With the development of new technology, advanced tools such as parametricization, big data, finite element analysis, and AI intelligence to enhance the understanding and application of MT joints in various contexts (Yue *et al*. 2024). These technologies allow for a more nuanced and detailed examination of the joints, enabling researchers to predict their performance under different stress conditions and to optimize their design for specific applications. The utilization of big data technologies has facilitated the collection and analysis of vast amounts of information related to MT joints. This data-driven approach provides insights into patterns and trends that may not be apparent through traditional research methods (Kasal *et al*. 2016; Zhang *et al*. 2023). It also aids in identifying potential areas for improvement and innovation. AI intelligence has also been integrated into the study of MT joints harnessing the power of machine learning and artificial neural networks to predict the behavior of these joints and to generate novel design solutions (Xue *et al*. 2021; Zhang and Hu 2021). In addition to these technological advancements, some studies have combined three-dimensional numerical model with physical experiments to validate the accuracy and feasibility of the virtual models (Wu *et al*. 2021a). Some researchers have applied finite element methods technologies to simulate and analyze the structural behavior of MT joints (Tankut *et al*. 2014; Kaygin *et al*. 2016; Hu and Guan 2019; Iraola *et al*. 2021).

Research on Classification of MT Joints

Although there are various studies on the structure and form of MT joints, research on the classification and indexing of MT morphologies is relatively scarce. The classification of mortise-and-tenon shapes is mainly based on the overall construction relationship of the mortise-and-tenon structure, the shape of the tenon, the number of tenons, the visibility of the tenons, and the openness of the mortises (Van *et al*. 2023). Ecke (1986) meticulously catalogued 34 types of mortise-and-tenon joints, encompassing a range of structures such as box, yoke, and slab constructions. Gary Rogowski (2002) have showcased the specific craftsmanship of dozens of mortise-and-tenon forms in their works, highlighting exemplary joint types from around the globe. Collectively, these studies have enriched our understanding of the diversity and craftsmanship inherent in mortise-and-tenon technology, providing a valuable knowledge base for the preservation and contemporary application of traditional joint techniques. Guan (2007) classified modern furniture joining methods into three categories: integral tenon jointing, separate tenon jointing, and connector jointing. Further subdivision of the first two categories yielded 12 types based primarily on tenon shape. Zhang and Yang (2018) categorized ancient architectural MT joints into three major classes and 11 subcategories. They also classified furniture component joining methods into three types: longitudinal extension jointing, transverse width jointing, and end-inlay jointing, listing 146 specific MT types. Chen (2014) divided traditional furniture MT joints into eight categories. Liang *et al*. (2021) classified Chinese traditional furniture MT forms into four categories.

The classification exhibits ambiguity in defining its boundaries, both internally and externally. There is currently no consensus on MT joint classification, as classifications may be limited by research focus, logic, or cultural tradition adherence. Additionally, specific MT styles may have diverse names across different cultures and regions. There is a need for further efforts in standardizing, systematizing, and universalizing taxonomic research in this area. Therefore, this study aims to develop a classification system for MT forms that draws from various taxonomic methodologies and research streams.

Current research on classification methods encompasses biological taxonomy, morphological classification, and information systems classification including, for instance, a method tailored for information systems classification (Nickerson *et al*. 2013; Kundisch *et al*. 2022). Chen *et al*. (2022) proposed an innovative method for automatically merging multiple source classifications into a target classification, addressing the complexities associated with multiple inheritance issues. Furthermore, De Queiroz (2006) sheds light on the distinctions between systematic coding, taxonomy, and nomenclature, offering valuable insights for delineating the conceptual boundaries of this study. Fischer and Gregor (2011) contributed to design science by proposing an idealized model of hypothesis deduction, enhancing fundamental reasoning forms. Building upon this literature analysis, this study will employ a spatial geometric interpretation of morphological classification, integrating principles from MT joints and wood characteristics. Drawing inspiration from biological classification methods and linear pairing algorithms, a systematic and universally applicable MT morphology classification index system will be formulated.

Classification Methodology

This study proposes a systematic classification method for MT joints based on connection forms. In this section, an index system for MT forms is established, where definitions and coding for MT classification are provided. Afterwards, the MT joint assessment research is carried out based on the MT principles and visual analysis.

The hierarchical structure of MT joints

Wood is primarily sourced from the main trunks of trees, with wood used by humans typically cut from these trunks into various profiles. This wood is categorized into scantlings and boards. Joint production, which involves the creation of interlocking joints, focuses on managing the connection between these materials. Figure 1 shows the classification of MT joints, based on biological classification principles and consisting of six hierarchical levels.

The definitions and coding for MT joints

This study focuses on morphological classification of MT joints, specifically targeting the fifth level of the hierarchical taxonomy, termed as Genus. It presents various categories of joint methods between components in different dimensions, without delving into the specific structural styles under the sixth level, termed as Species. The following outlines the specific definitions and coding schemes for the aforementioned taxonomy.

According to the definition of surface and scantlings from the Chinese Forestry Industry Standard LY/T 1788-2023 (2023), the width-to-thickness ratio R can be calculated by Eq. 1,

$$R = W / T \tag{1}$$

where W and T represent the width and the thickness, respectively, of the timber component.

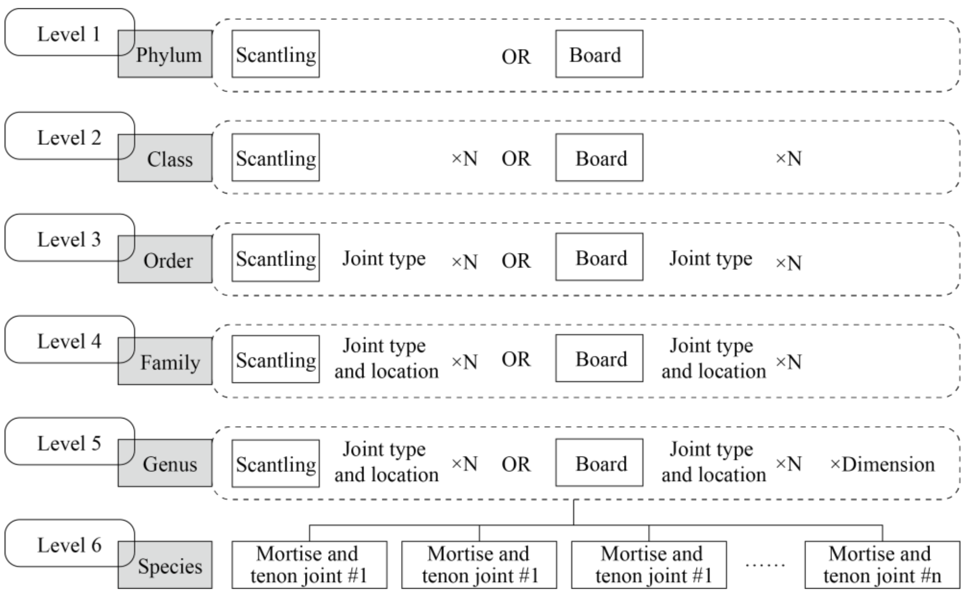

Fig. 1. The hierarchical structure of MT joints
1) Phylum: distinguishes between scantlings and boards.
2) Class: identifies the types and quantities of components involved.
3) Order: categorizes various junction point elements for scantlings and boards.
4) Family: distinguishes between different joining methods for component junction points.
5) Genus: categorizes structural variants of joining methods.
6) Species: encompasses specific structural styles derived from each joining method variant.

At the Phylum level, if $R < 2$, the component can be categorized as scantlings, while those with $R \geqslant 2$ are categorized as boards. In Figure 2a, Scantling has cross-sectional dimensions where area is not considered, and its length is variable within limits. The board's length and width can also vary within limits. In real-life practice, there may be curved components, which can be classified into categories of scantlings and boards based on their cross-sectional dimensional ratios, shown in Fig. 2b. When denoting scantling as L and board as F. Three relationships between two components: scantling to scantling (L), board to board (F), and scantling to board (L&F).

At the Class level, all component junctions are aggregated into one structural point or line, and multiple components' multiple junction points are separately categorized. Each component participating in the structure is represented within three dimensions – transverse, longitudinal, and diagonal, let *x*, *y*, *z* represent to the corresponding axis, respectively. Thus, the number of components involved is limited to a maximum of three, and multiple structural elements in the same dimension are treated as one component. As is shown in Fig. 2c, based on this setup, the joint between scantlings and boards can be classified into seven types: *L*+*L*, *L*+*L*+*L*, *F*+*F*, *F*+*F*+*F*, *L*+*F*, *L*+*L*+*F*, and *L*+*F*+*F*.

At the Order level, scantling can be categorized into two types of cross-sectional junction elements: cross-section (*c*) and lateral side (*s*). Surface material can be categorized into three types of junction elements: end face (*e*), long side (*a*), and surface (*p*).

At the Family level, as is shown in Fig. 2d, scantling's cross-section has only one joint, denoted as L_c, whereas its lateral side has two types of joints: lateral side head (L_{s1}) and lateral side middle (L_{s2}). Surface material's end face has two types of junction points: end face head (F_{e1}) and end face middle (F_{e2}), long side has two types: long side head (F_{a1}) and long side middle (*Fa*2), and surface has four types: surface end head (F_{p1}), surface end middle (F_{p2}), surface side middle (F_{p3}), and surface center (F_{p4}).

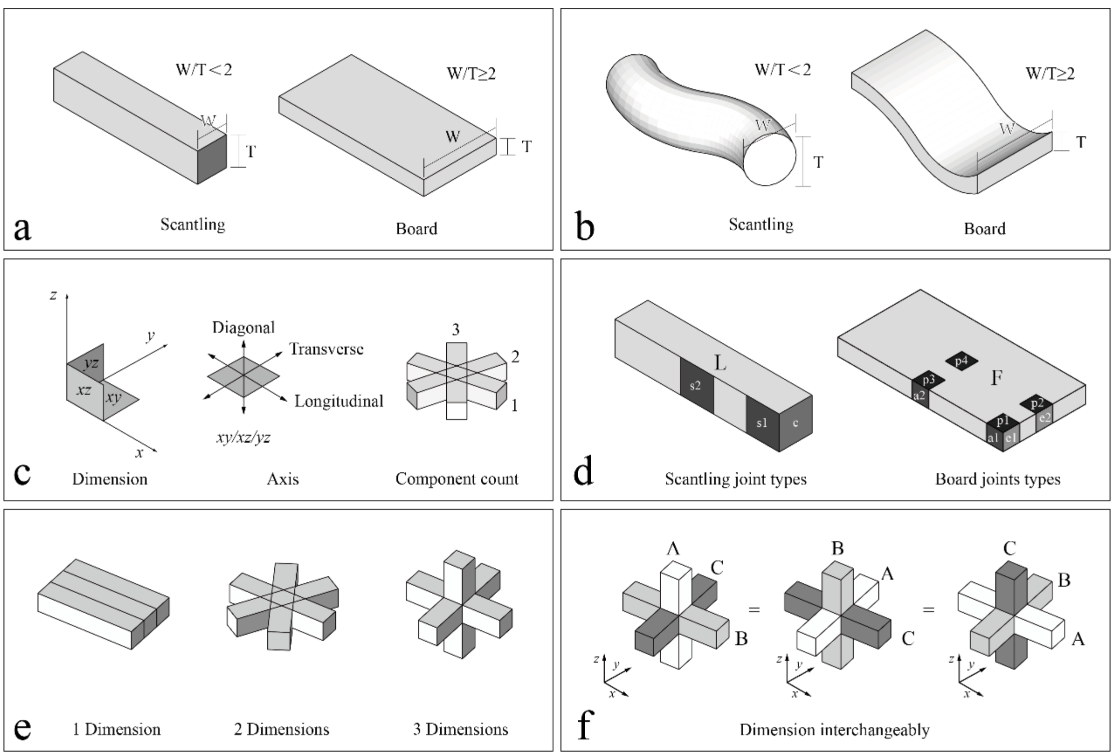

Fig. 2. MT joint coding. (a) Categories of scantlings and boards based on their cross-sectional dimensional ratios; (b) Curved components classification; (c) Definition of dimension, axis and component count; (d) Joint types; (e) Component joint by different dimensions; (f) Dimension interchangeably

At the Genus level, as is shown in Fig. 2e, the classification methods between components are further categorized into three types: one-dimensional linear joint (*x*), two-dimensional angular joint (*x*-*y*), and three-dimensional angular joint (*x*-*y*-*z*). Each type of joint may have multiple variants in the three different dimensions. Because the components are considered standard, their positions can be interchanged within the three-dimensional plane after joining without affecting the structural integrity. Thus, the variety of joint methods can be reduced by eliminating redundant combinations, shown in Fig. 2f. These classifications provide a comprehensive framework for understanding and categorizing joint methods in a systematic manner.

The MT Joint Classification Process

Based on the definitions of classification methods across five hierarchical levels, we combine component joint and dimension coding to deduce potential MT joint compositions. Using the example of an *L+F* joint formed by one board component and one scantling component at the Class level, illustrate the specific classification inference and coding steps.

Step 1: Phylum

As per the definitions provided, an *L+F* joint at the Class level belongs to the category of scantling-board joints at the Phylum level.
Example: Resulting Phylum-level classification code: *L&F*

Step 2: Class
Example: Class-level classification code: *L+F*

Step 3: Order
There are two types of joint elements, shown as formular (2).

$$\begin{cases} L = L_c + L_s & \text{for scantling} \\ F = F_e + F_a + F_p & \text{for board} \end{cases} \tag{2}$$

Using arithmetic cross-multiplication, simple linear pairing of joints is performed.
Example: Resulting Order-level classification code: *ce*, *ca*, *cp*, *se*, *sa*, *sp*

Step 4: Family

As mentioned before, scantling has only one junction point for its cross-section, and two for its lateral side. Similarly conditions are met for board components. Then we have

$$\begin{cases} L_c = L_c \\ L_s = L_{s1} + L_{s2} \\ F_e = F_{e1} + F_{e2} \\ F_a = F_{a1} + F_{a2} \\ F_p = F_{p1} + F_{p2} + F_{p3} + F_{p4} \end{cases} \tag{3}$$

Hence, all possible combinations of joint points can be represented as

$$\sum_{LF} = \sum\left(L_c + L_{s1} + L_{s2}\right)\left(F_{e1} + F_{e2} + F_{a1} + F_{a2} + F_{p1} + F_{p2} + F_{p3} + F_{p4}\right) \tag{4}$$

Example: Arrive at the Family-level classification code, resulting in 24 classes.

Step 5: Genus

Building upon the combinations of joint points, the three-dimensional elements as is shown in Fig. 2e are incorporated.
This can be represented as

$$\sum_{LF(xyz)} = \sum\left(L_c + L_{s1} + L_{s2}\right)\left(F_{e1} + F_{e2} + F_{a1} + F_{a2} + F_{p1} + F_{p2} + F_{p3} + F_{p4}\right)\left(x + xy + xyz\right) \tag{5}$$

Expanding this, the Genus-level classification code is obtained, as detailed in Table 1.
Example: Based on Table 1, it can be inferred that the *L+F* joint formation between a

single scantling component and a single board component yields theoretically 72 types of joint formations.

Following the calculation method above, all seven types of joints between scantlings and boards at the Class level are expanded. Among them, combinations involving similar components (such as *F*+*F*, *L*+*L*+*F*, *etc*.) need to adhere to the principle of interchangeable components, as is shown in Fig. 2f, reducing redundant joint formations in the encoding.

As the Phylum level and the Class level concentrate to the style of the components while the Order level, the Family level and the Genus level focus on the connection, the label of a MT joint can be marked by connecting two labels. Label 1 denotes the detail of Phylum level and the Class level, and Label 2 denotes the Order level, the Family level and the Genus level, as shown as Fig. 3.

Table 1. Scantling-Board Joint (*L*+*F*) Inferred Classification Code

No.	Phylum	Class	Order	Family	Genus		
					1 Dimension	2 Dimensions	3 Dimensions
1	*L&F*	*L+F*	*ce*	*ce*1	*ce*1*x*	*ce*1*xy*	*ce*1*xyz*
2				*ce*2	*ce*2*x*	*ce*2*xy*	*ce*2*xyz*
3			*ca*	*ca*1	*ca*1*x*	*ca*1*xy*	*ca*1*xyz*
4				*ca*2	*ca*2*x*	*ca*2*xy*	*ca*2*xyz*
5			*cp*	*cp*1	*cp*1*x*	*cp*1*xy*	*cp*1*xyz*
6				*cp*2	*cp*2*x*	*cp*2*xy*	*cp*2*xyz*
7				*cp*3	*cp*3*x*	*cp*3*xy*	*cp*3*xyz*
8				*cp*4	*cp*4*x*	*cp*4*xy*	*cp*4*xyz*
9			*se*	*s*1*e*1	*s*1*e*1*x*	*s*1*e*1*xy*	*s*1*e*1*xyz*
10				*s*1*e*2	*s*1*e*2*x*	*s*1*e*2*xy*	*s*1*e*2*xyz*
11				*s*2*e*1	*s*2*e*1*x*	*s*2*e*1*xy*	*s*2*e*1*xyz*
12				*s*2*e*2	*s*2*e*2*x*	*s*2*e*2*xy*	*s*2*e*2*xyz*
13			*sa*	*s*1*a*1	*s*1*a*1*x*	*s*1*a*1*xy*	*s*1*a*1*xyz*
14				*s*1*a*2	*s*1*a*2*x*	*s*1*a*2*xy*	*s*1*a*2*xyz*
15				*s*2*a*1	*s*2*a*1*x*	*s*2*a*1*xy*	*s*2*a*1*xyz*
16				*s*2*a*2	*s*2*a*2*x*	*s*2*a*2*xy*	*s*2*a*2*xyz*
17			*sp*	*s*1*p*1	*s*1*p*1*x*	*s*1*p*1*xy*	*s*1*p*1*xyz*
18				*s*1*p*2	*s*1*p*2*x*	*s*1*p*2*xy*	*s*1*p*2*xyz*
19				*s*1*p*3	*s*1*p*3*x*	*s*1*p*3*xy*	*s*1*p*3*xyz*
20				*s*1*p*4	*s*1*p*4*x*	*s*1*p*4*xy*	*s*1*p*4*xyz*
21				*s*2*p*1	*s*2*p*1*x*	*s*2*p*1*xy*	*s*2*p*1*xyz*
22				*s*2*p*2	*s*2*p*2*x*	*s*2*p*2*xy*	*s*2*p*2*xyz*
23				*s*2*p*3	*s*2*p*3*x*	*s*2*p*3*xy*	*s*2*p*3*xyz*
24				*s*2*p*4	*s*2*p*4*x*	*s*2*p*4*xy*	*s*2*p*4*xyz*

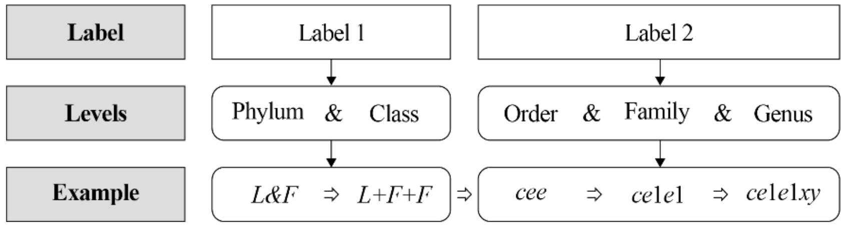

Fig. 3. The code of a single MT joint

Through deduction, 352 types of Family-level joint formations and 1056 types of Genus-level joint formations can be obtained, as shown in Table 2.

Table 2. The MT Joints Sequence

No.	Label 1		Label 2				
	Phylum	Class	Order	Family	Genus		
					1 Dimension	2 Dimensions	3 Dimensions
1	*L*	*L+L*	*cc*	*cc*	*ccx*	*ccxy*	*ccxyz*
2			*cs*	*cs*1	*cs*1*x*	*cs*1*xy*	*cs*1*xyz*
3				*cs*2	*cs*2*x*	*cs*2*xy*	*cs*2*xyz*
4			*ss*	*s*1*s*1	*s*1*s*1*x*	*s*1*s*1*xy*	*s*1*s*1*xyz*
5				*s*1*s*2	*s*1*s*2*x*	*s*1*s*2*xy*	*s*1*s*2*xyz*
6				*s*2*s*2	*s*2*s*2*x*	*s*2*s*2*xy*	*s*2*s*2*xyz*
7		*L+L+L*	*ccc*	*ccc*	*cccx*	*cccxy*	*cccxyz*
8			*ccs*	*ccs*1	*ccs*1*x*	*ccs*1*xy*	*ccs*1*xyz*
9				*ccs*2	*ccs*2*x*	*ccs*2*xy*	*ccs*2*xyz*
10			*css*	*cs*1*s*1	*cs*1*s*1*x*	*cs*1*s*1*xy*	*cs*1*s*1*xyz*
11				*cs*1*s*2	*cs*1*s*2*x*	*cs*1*s*2*xy*	*cs*1*s*2*xyz*
12				*cs*2*s*2	*cs*2*s*2*x*	*cs*2*s*2*xy*	*cs*2*s*2*xyz*
13			*sss*	*s*1*s*1*s*1	*s*1*s*1*s*1*x*	*s*1*s*1*s*1*xy*	*s*1*s*1*s*1*xyz*
14				*s*1*s*1*s*2	*s*1*s*1*s*2*x*	*s*1*s*1*s*2*xy*	*s*1*s*1*s*2*xyz*
15				*s*1*s*2*s*2	*s*1*s*2*s*2*x*	*s*1*s*2*s*2*xy*	*s*1*s*2*s*2*xyz*
16				*s*2*s*2*s*2	*s*2*s*2*s*2*x*	*s*2*s*2*s*2*xy*	*s*2*s*2*s*2*xyz*
…	…		…				
349	*L&F*	*L+F+F*	*spp*	*s*2*p*2*p*4	*s*2*p*2*p*4*x*	*s*2*p*2*p*4*xy*	*s*2*p*2*p*4*xyz*
350				*s*2*p*3*p*3	*s*2*p*3*p*3*x*	*s*2*p*3*p*3*xy*	*s*2*p*3*p*3*xyz*
351				*s*2*p*3*p*4	*s*2*p*3*p*4*x*	*s*2*p*3*p*4*xy*	*s*2*p*3*p*4*xyz*
352				*s*2*p*4*p*4	*s*2*p*4*p*4*x*	*s*2*p*4*p*4*xy*	*s*2*p*4*p*4*xyz*

Typicality Assessment for the Classified MT Joints

Wood exhibits anisotropic properties, meaning that its physical characteristics vary significantly across different grain orientations. Due to this and various factors such as form, structure, scale, and application scenarios, the application of MT joints in real-life settings may be constrained. Joint production addresses these variations to optimize mechanical strength, adhesive performance, dimensional stability, processing feasibility, and aesthetic appeal. The structure forms derived from theoretical deductions based on formative composition may manifest differently in practical scenarios, necessitating the classification and practical application assessment.

The structures can be categorized into three scenarios:
1) Non-existent joint. These violate the basic principles of MT joints and lack practical application examples, marked with "*N*".
2) Atypical joint. Although theoretically possible, these are rarely observed in real-life scenarios, marked with "*U*".
3) Typical joint. These joints are logically sound and either have practical applications or existing case studies, marked with "*C*".

Visual analysis a commonly utilized information analysis method, combines human visual exploration capabilities with computer processing power. By converting symbols into geometric shapes, researchers can visually observe computer simulations and calculations, making scientific research more intuitive and possibly uncovering unexpected discoveries (Averbukh 2001). To facilitate a more intuitive classification, 3D models are employed to visualize and simulate all joint formations listed in Table 3, generating specific graphical representations for various MT joint forms, as illustrated in Table 4.

By systematically modeling each of the MT joint forms listed in Table 3, a total of 508 visually intuitive virtual representations of joint types are obtained. In Table 4, symbol N/A represents the schematic diagram is not available, include two conditions.

Condition 1, nonexistent in such scenarios. It is observed that certain joint forms could not be simulated through computer graphics, indicating their non-existence in reality. For instance, the combination of two components cannot form a three-dimensional joint, so as three-dimensional joint types nonexistent in such scenarios.

Condition 2, does not match the requirement. Some joint methods could be graphically represented but violated previously specified constraints. For example, once Label 1 is *L+L+L* and Label 2 is *cccx*, involving repetitive dual-plane joints, contradicts the requirement of unique joint points as defined earlier and thus needs to be excluded.

Following this simulation and mapping process, a total of 548 inferred joint types from Table 3 are excluded, including *ccxyz*, *e*1*e*2*a*1*xy*, *cp*3*x*, *s*2*s*2*p*3*x*, *s*1*a*1*p*4*x*, among others.

For MT joint types that can be simulated through graphics, further assessment of their typicality and practical applicability in real-life scenarios is necessary. While some joint forms may theoretically allow for viable joints, their practical utility could be constrained by various factors such as morphology, structure, space, scale, wood characteristics, and application contexts, as outlined below:

1) As is shown in Fig. 4a, due to the uncertain extendibility of scantlings and boards, certain joint forms may have limitations in practical applications, necessitating judgment of their typicality based on real-world conditions.

2) Although some simulated MT joint types may exhibit identical or similar joint forms under approximate scaling of simulated components, their dimensional differences upon expansion need to be manually assessed to determine typical joint forms, the schematic diagram is shown in Fig. 4b.

3) Wood's poor transverse tensile and shear resistance may limit the use of certain joint types as structural components. On the contrary, as is shown in Fig. 4c, with appropriate scaling of tenon dimensions, their strength may meet general usage requirements, rendering them as typical MT joint types in certain cases.

4) While the edge-to-edge joint of scantlings is typically substituted with surface-to-surface

joint of board in practice, this type may still find application in specific scenarios and can be considered typical forms, as illustrated in Fig. 4d.

5) The anisotropic nature of wood, along with differences in component angles or wood grain direction, significantly affects the joint strength of MT joints (Xie *et al*. 2021). Additionally, differential swelling and shrinking properties between end-grain and long-grain surfaces may render certain joint forms less feasible at larger component scales but still viable at smaller scales, as shown in Fig. 4e.

6) As shown in Fig. 4f, while theoretically diverse, three-dimensional jointing involving multiple boards may have limited practical applications, with the majority considered as atypical joint forms.

7) In Fig. 4g, component scaling extending towards different-dimensional surfaces may generate an interference zone, rendering such joint forms less typical.

8) Certain simulated joint forms, while theoretically featuring joint points, may exhibit peculiar aesthetics or deviate from customary usage practices, as is shown in Fig. 4h. The joints are regarded as atypical joint forms.

Table 3. Visual Analysis Classification Schematic Diagrams

Label 1	Label 2 1 Dimension	Schematic diagram	Label 2 2 Dimensions	Schematic diagram	Label 2 3 Dimensions	Schematic diagram
L+L	*ccx*	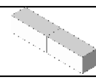	*ccxy*	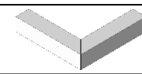	*ccxyz*	N/A
	*cs*1*x*	N/A	*cs*1*xy*	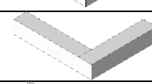	*cs*1*xyz*	N/A
	*cs*2*x*	N/A	*cs*2*xy*	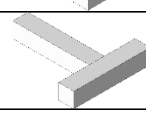	*cs*2*xyz*	N/A
	*s*1*s*1*x*	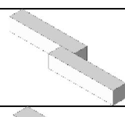	*s*1*s*1*xy*	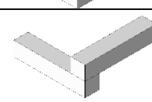	*s*1*s*1*xyz*	N/A
	*s*1*s*2*x*	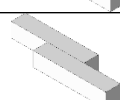	*s*1*s*2*xy*	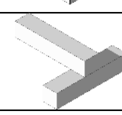	*s*1*s*2*xyz*	N/A
	*s*2*s*2*x*	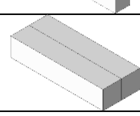	*s*2*s*2*xy*	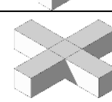	*s*2*s*2*xyz*	N/A
L+L+L	*cccx*	N/A	*cccxy*	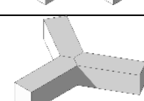	*cccxyz*	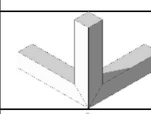
	*ccs*1*x*	N/A	*ccs*1*xy*	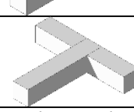	*ccs*1*xyz*	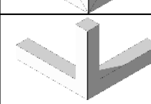
	*ccs*2*x*	N/A	*ccs*2*xy*	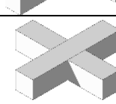	*ccs*2*xyz*	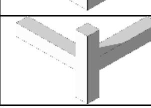
……						
L+F+F	*s*2*p*2*p*4*x*	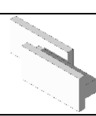	*s*2*p*2*p*4*xy*	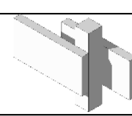	*s*2*p*2*p*4*xyz*	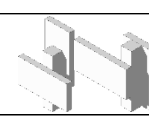

	s2p3p3x	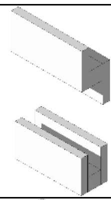	*s2p3p3xy*		*s2p3p3xyz*	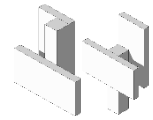 ……
	s2p3p4x	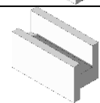	*s2p3p4xy*	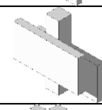	*s2p3p4xyz*	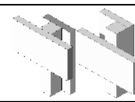
	s2p4p4x		*s2p4p4xy*	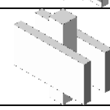	*s2p4p4xyz*	

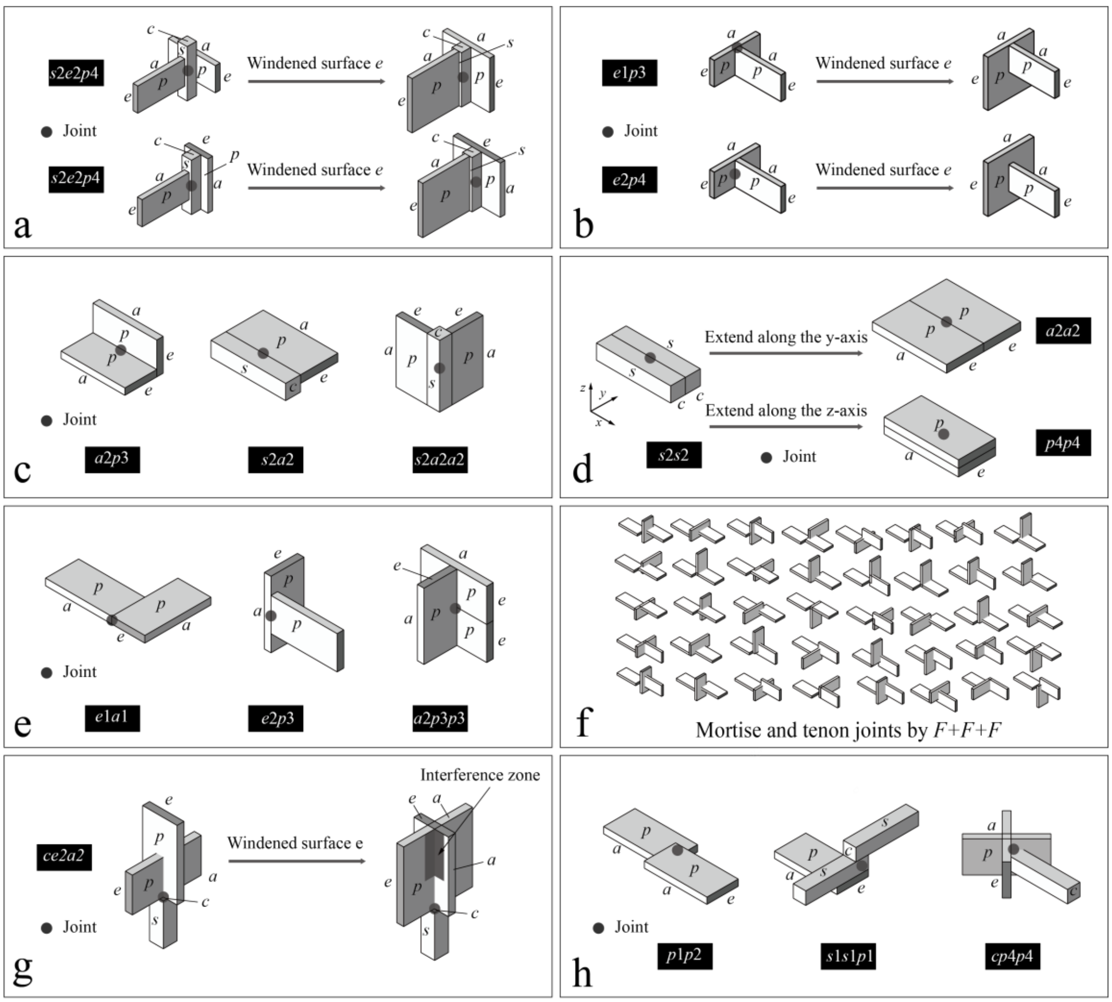

Fig. 4. Factors considered in MT classification
(a) The impact of component scale variation on joint morphology; (b) MT joints with similar forms but different joint points; (c) Joint forms where tenons are cut across the wood grain; (d) Evolution and application of jointing where line materials are joined at their edges; (e) Joint forms where wood grain directions intersect; (f) The theoretical richness of joint forms involving multiple boards; (g) Interference potentially caused by component scale extension, particularly concerning dimensional surface interference; (h) Some theoretically derived joint forms with peculiar aesthetics.

These restrictions aim to discern the typology and practical viability of simulated MT joint forms.

Table 4. Assessment Results of MT Joint Types

No.	Label 1	Label 2 1 Dimension	Assessment result	Label 2 2 Dimensions	Assessment result	Label 2 3 Dimensions	Assessment result
1	*L+L*	*ccx*	*C*	*ccxy*	*C*	*ccxyz*	*N*
2		*cs1x*	*N*	*cs1xy*	*C*	*cs1xyz*	*N*
3		*cs2x*	*N*	*cs2xy*	*C*	*cs2xyz*	*N*
4		*s1s1x*	*U*	*s1s1xy*	*U*	*s1s1xyz*	*N*
5		*s1s2x*	*U*	*s1s2xy*	*U*	*s1s2xyz*	*N*
6		*s2s2x*	*C*	*s2s2xy*	*C*	*s2s2xyz*	*N*
7	*L+L+L*	*cccx*	*N*	*cccxy*	*C*	*cccxyz*	*C*
8		*ccs1x*	*N*	*ccs1xy*	*C*	*ccs1xyz*	*C*
9		*ccs2x*	*N*	*ccs2xy*	*C*	*ccs2xyz*	*C*
10		*cs1s1x*	*N*	*cs1s1xy*	*C*	*cs1s1xyz*	*C*
11		*cs1s2x*	*N*	*cs1s2xy*	*N*	*cs1s2xyz*	*U*
12		*cs2s2x*	*N*	*cs2s2xy*	*U*	*cs2s2xyz*	*C*
13		*s1s1s1x*	*U*	*s1s1s1xy*	*U*	*s1s1s1xyz*	*C*
14		*s1s1s2x*	*U*	*s1s1s2xy*	*U*	*s1s1s2xyz*	*C*
15		*s1s2s2x*	*U*	*s1s2s2xy*	*U*	*s1s2s2xyz*	*U*
16		*s2s2s2x*	*C*	*s2s2s2xy*	*C*	*s2s2s2xyz*	*C*
……							
349	*L+F+F*	*s2p2p4x*	*U*	*s2p2p4xy*	*U*	*s2p2p4xyz*	*U*
350		*s2p3p3x*	*C*	*s2p3p3xy*	*C*	*s2p3p3xyz*	*U*
351		*s2p3p4x*	*C*	*s2p3p4xy*	*U*	*s2p3p4xyz*	*C*
352		*s2p4p4x*	*C*	*s2p4p4xy*	*C*	*s2p4p4xyz*	*C*

Table 5. Summary of the Assessment Results

Phylum	Class	Order	Family	Genus			
				Total	N/A	Atypical (*U*)	Typical (*C*)
L	*L+L*	3	6	18	8	4	6
	L+L+L	4	10	30	7	9	14
F	*F+F*	6	36	108	56	33	19
	F+F+F	10	120	360	265	78	17
L&F	*L+F*	6	24	72	36	8	28
	L+L+F	9	48	144	43	51	50
	L+F+F	12	108	324	133	127	64
Sum	7	50	352	1056	548	310	198

Table 6. Typical MT Joints

No.	Label 1	Label 2	schematic diagram	No.	Label 1	Label 2	schematic diagram
1	*L+L*	*ccx*	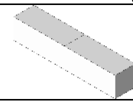	11	*L+L+L*	*ccs2xy*	
2	*L+L*	*ccxy*	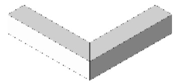	12	*L+L+L*	*ccs2xyz*	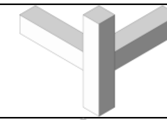
3	*L+L*	*cs1xy*	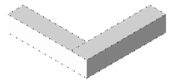	13	*L+L+L*	*cs1s1xy*	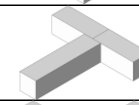
4	*L+L*	*cs2xy*	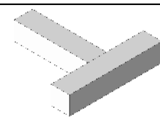	14	*L+L+L*	*cs1s1xyz*	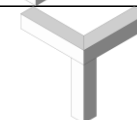
5	*L+L*	*s2s2x*	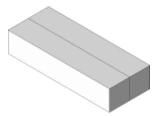	15	*L+L+L*	*cs2s2xyz*	
6	*L+L*	*s2s2xy*	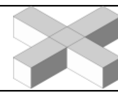			……	
7	*L+L+L*	*cccxy*	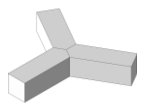	195	*L+F+F*	*s2p3p4xyz*	
8	*L+L+L*	*cccxyz*	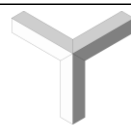	196	*L+F+F*	*s2p4p4x*	
9	*L+L+L*	*ccs1xy*	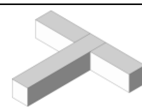	197	*L+F+F*	*s2p4p4xy*	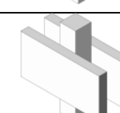
10	*L+L+L*	*ccs1xyz*	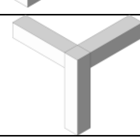	198	*L+F+F*	*s2p4p4xyz*	

Regarding the issue of the typicality of MT joint types under various real-world conditions, it requires manual assessment considering multiple factors. To this end, the authors invited 11 experts in the field and experienced frontline workers to evaluate the aforementioned 508 MT joint types that could be simulated through computer modeling. Based on the majority principle, two assessment results are provided: typical (*C*) and atypical (*U*), as shown in Table 4. The summary of the assessment results is shown in Table 5. Some typical MT joints are shown in Table 6.

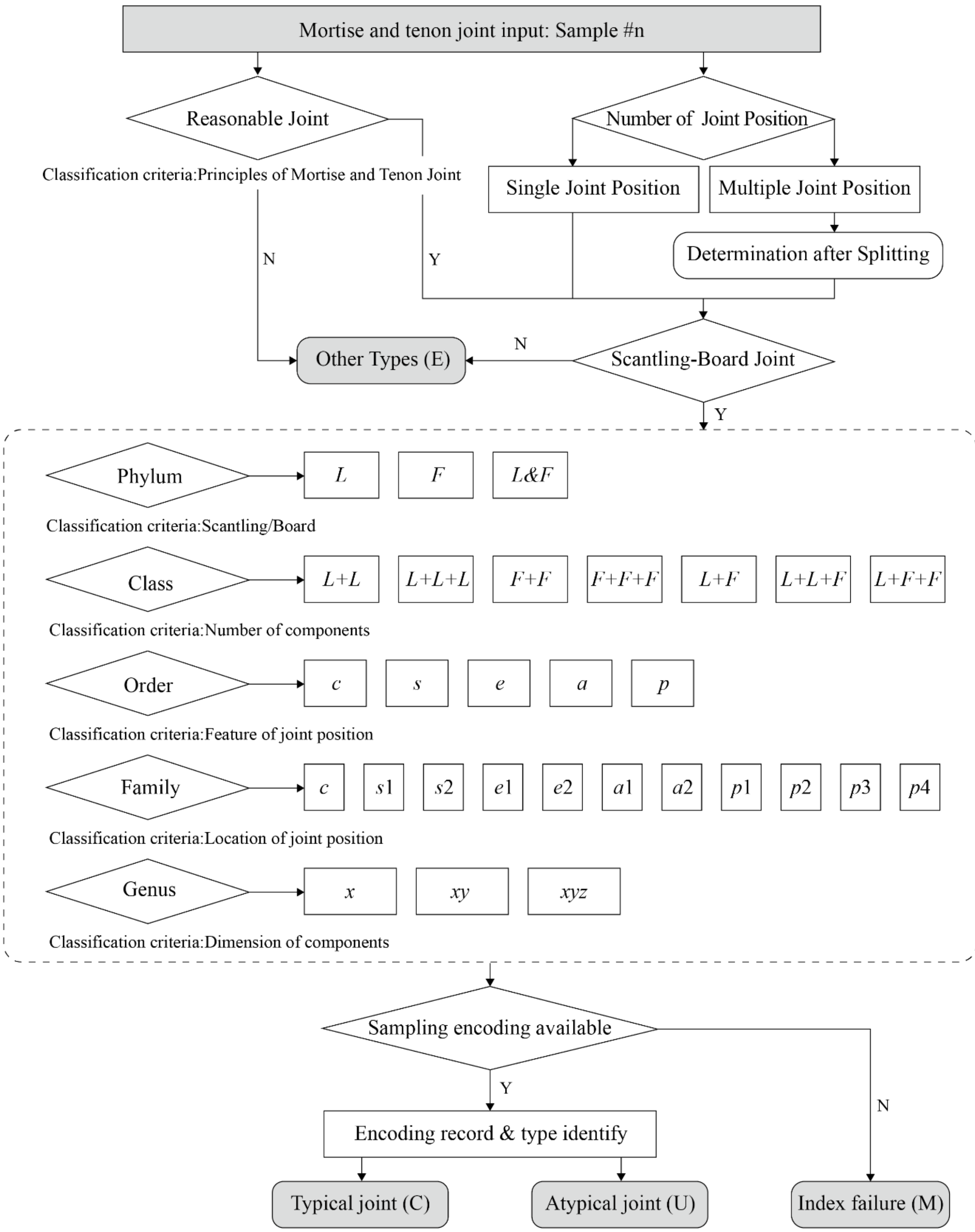

Fig. 5. Validation method for MT sampling, coding, and classification

Classification and Assessment Practice

Classification and assessment process

To validate the MT joint classification and assessment method, thousands of MT joints were collected from 3210 internet images, 17 relevant books, 223 videos on MT production or demonstration, and 622 research articles. After removing duplicate samples, a total of 2,654 clearly identified and distinct MT joint cases have been obtained.

Following the proposed method, features of the collected samples are determined through team discussions and expert consultations, these samples are then encoded to examine the feasibility of the coding and validate the assessment status of the MT types attributed by the coding. Samples that could not be accurately encoded are marked as *M*. It is observed that some MT samples did not exhibit scantling or board structure but still demonstrated characteristics of MT joints.

These forms are primarily decorative or reinforcement structures, not main structural components bearing significant mechanical loads. Additionally, some MT cases exhibited clear structural design flaws and could not be considered as reasonable MT forms. These samples are categorized as other types and marked as *E*. The basic determination process is outlined in Fig. 5.

Based on the approach outlined in Fig. 5, individual analysis and classification of MT joint samples were conducted. Table 7 provides examples of the classification results for some of the samples.

Assessments and determinations are completed for all sampling cases mentioned above. As shown in Fig. 6, 98.5% of 2654 sampled MT joint cases can be encoded. This demonstrates that the coding system and evaluation results of this index hierarchy have a high level of credibility. The proposed method is a feasible way to classify the MT joints.

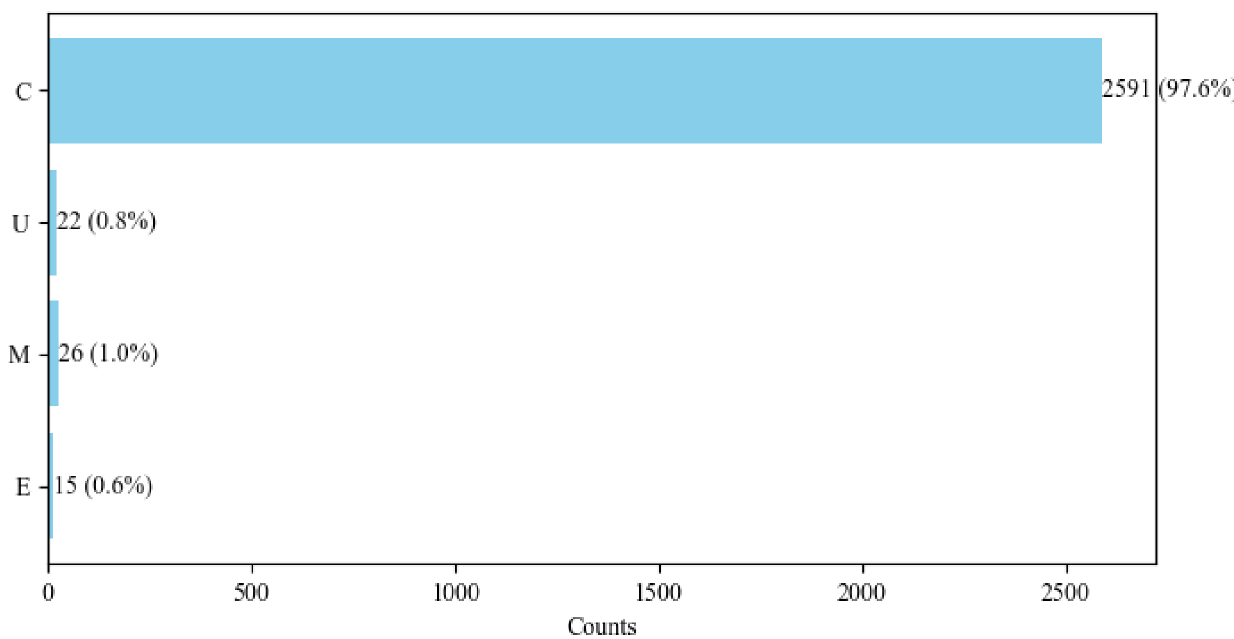

Fig. 6. Proportion of samples

Table 7. Samples of MT Sampling Classification Analysis

Figure					
Judging Criteria	Boards End Joint Miter Joint	Scantling and board End Joint Edge-to-Edge Joint, Miter Joint	Scantlings Multiple Components Line Cross Joint Plane Joint	Scantlings Multiple Material Cross Joint Three-Dimensional Joint	Boards End Joint Plane Joint
Phylum	*F*	*F*	*L&F*	*L*	*F*
Class	*F+F*	*F+F*	*L+F+F*	*L+L+L*	*F+F*
Order	*ee*	*ee*	*see*	*sss*	*ea*
Family	*e2e2*	*e2e2*	*s2e2e2*	*s2s2s2*	*e2a2*
Genus	*e2e2xy*	*e2e2xy*	*s2e2e2xyz*	*s2s2s2xy*	*e2a2x*
Assessment	*C*	*C*	*C*	*C*	*U*
Figure			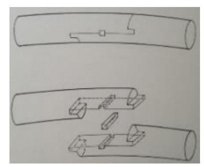	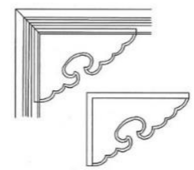	
Judging Criteria	Boards Edge Joint Sloped Miter Joint	Curved scantlings Circular Diameter Linear Joint	Scantlings End joint Miter Joint	Boards End Edge Joint Plane Joint	Scantlings Decoration Use
Phylum	*L*	*F*	*L*	*L*	*L*
Class	*L+L+L*	*F+F+F*	*L+L*	*L+L*	*L+L*
Order	*css*	—	*cc*	*cc*	—
Family	*cs2s2*	—	*cc*	*cc*	—
Genus	*cs2s2xyz*	—	*ccx*	*ccxy*	—
Assessment	*C*	*M*	*C*	*C*	*E*

Note: *C* indicates that the case is a typical mortise-and-tenon structure; *U* indicates that the case is an atypical mortise-and-tenon structure; *M* indicates that the case cannot be encoded; *E* indicates that the case belongs to another category.

Discussion

The current academic approach to defining MT types mostly relies on the morphological division of existing MT joints, which belongs to qualitative research characterized by summarization and induction. Due to the diversity of MT joints and their widespread applications, these classification methods often lack comprehensiveness and systematicity. This study takes the paradigm of morphological composition as the starting point, focusing on the most basic forms of components used for making MT joints, rather than the final forms presented by wooden products. In the classification hierarchy, a well-known biological classification system is adopted, and the encoding deduction method utilizes scientific arithmetic cross-algorithm. Therefore, it is proposed here that the MT index hierarchy constructed in this paper is logically rigorous, systematic, more compatible, and capable of inferring almost all existing and future MT joint types. As tools, equipment, and MT skills continue to advance, new forms of MT joints will emerge. The MT morphology classification index and coding system constructed in this paper can accommodate most new types of MT joints.

The sampled cases in the case study section of this paper represent MT morphologies deciphered from various sources worldwide and from various literature over several years, showing good coverage and representativeness. By comparing and analyzing the types of MT joints in real-life scenarios with the index hierarchy proposed in this paper, it can be observed where some types of MT morphologies are insufficiently applied or studied in reality. This helps promote innovation in MT joint morphologies under certain classifications, improve specific MT structural styles, and enrich the database of MT structural styles.

The MT morphology classification index hierarchy constructed in this paper facilitates users to conveniently access and retrieve MT style resources, making it more universal and conducive to communication and exchange among users with different language backgrounds and in different geographical environments. It helps users in related fields to innovate based on this foundation, cite, reference, or innovate further, meet diverse demands, and be widely applied in the fields of architectural design, furniture design, cultural and creative industries, handicrafts, toys, and other wooden product design and production areas. Additionally, it provides certain reference or guidance value for researchers and frontline practitioners in related disciplines.

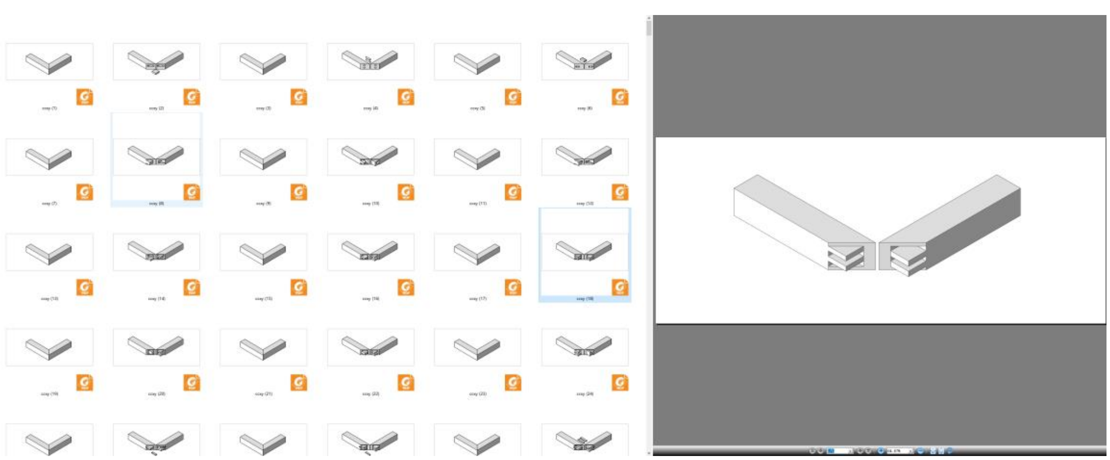

Fig. 7. Samples from the MT library

It should be noted that while the practice phase in this paper includes a considerable number of samples and has broad coverage, it cannot exhaust all current and future types of MT joints, especially those not included in the main hierarchy. Continuous verification and attention to the progress of MT research are required to further improve the hierarchy. Additionally, this paper does not delve into the species level in the index hierarchy, which refers to the specific joint styles of each type of MT joint. As shown in Fig. 7, by modeling, reproducing, or innovatively designing joint styles for 50 types of MT joints among the 198 typical morphologies mentioned above, a database of 7447 MT styles was established.

The paper proposes a systemic classification method for the MT joints, but the category phase is maintained within the limits for efficiency. Future work aims to provide a smart solution for the MT joint classification by integrating machine learning and intelligent recognition technology, and thereby exploring specific MT style design methods.

CONCLUSIONS

1. The paper used the paradigm of morphological composition as its starting point, based on the fundamental principles of mortise and tenon (MT) joints and the characteristics of wood, among other factors. It employed biological classification methods and arithmetic cross-method coding to establish a 6-level classification index hierarchy of MT morphology. By encoding the dimensions of MT joint points and morphological composition, the paper described 352 possible MT joint types and 1056 theoretical morphological compositions across multiple dimensions. This effectively demonstrated the structural logic of different MT morphologies, facilitating understanding and memorization.
2. A feasibility assessment of the morphological types under this hierarchy identified 198 typical and 310 atypical MT morphological types, with graphical representations for each. To validate the scientific and logical construction of this index hierarchy, 2654 research cases were analyzed. After extracting features from these cases, they were encoded based on the index hierarchy constructed in the paper. Thus, construction of this index hierarchy is feasible.

ACKNOWLEDGMENTS

This work is supported by the Humanities and Social Sciences Youth Foundation, Ministry of Education of the People's Republic of China (22YJCZH142) awarded to Bin Shang.

Author Contributions

Conceptualization: All authors; Methodology: BIN SHANG; Data collection: BIN SHANG and YUXI LIN; Data Analysis: BIN SHANG and HONG CHANG; Writing – original draft preparation: BIN SHANG, ZHE CHEN and JIANING WEI; Writing – review and editing: ZHE CHEN; Funding acquisition: BIN SHANG.

Ethical Approval

This article does not contain any studies with human participants or animals performed by any of the authors.

Conflict of Interest

The authors declare that they have no conflict of interest.

Informed Consent

No informed consent is required, because the data are anonymized.

Data Availability Statement

The data that supports the findings of this study are available in the supplementary material of this article.

REFERENCES CITED

Averbukh, V. L. (2001). "Visualization metaphors," *Programming and Computer Software* 27(5), 227-237. DOI: 10.1023/A:1012333025189

Bragança, L., Koukkari, H., Veljkovic, M., and Borg, R. P. (2010). "Sustainable construction- a life cycle approach in engineering," in: Proceedings, International Symposium Malta, 23-25 July 2010. COST Action C25. University of Malta, Faculty for the Built Environment.

Branco, J. M., and Descamps, T. (2015). "Analysis and strengthening of carpentry joints," *Construc. Build. Mater.* 97, 34-47. DOI: 10.1016/j.conbuildmat.2015.05.089

Chen, M., Wu, C., Yang, Z., Liu, S., Chen, Z., and He, X. (2022). "A multi-strategy approach for the merging of multiple taxonomies," *Journal of Information Science* 48(3), 283-303. DOI: 10.1177/0165551520952340

Chen, Y. (2014). "Tenon joint structure of Chinese traditional furniture (1) (in Chinese)," *Furniture & Interior Design* (3), 26-29. DOI: 10.16771/j.cnki.cn43-1247/ts.2014.03.003

Chinese Forestry Industry Standard LY/T 1788-2023. (2023). *Vocabulary of Wood Properties*. Beijing: Standards Press of China.

Claus, T., and Seim, W. (2020). "Tenon connections in timber constructions - fracture mechanic analysis and proposal of a new design model," *Bautechnik* 97, 76-+. DOI: 10.1002/bate.202000074

Darwesh, N., Hassan, R., Dzulkifli, A. R., Kudus, S. A., Noh, N. M., Shakimon, M. N., Zainal, A. A., and Anshari, B. (2024). "Experimental and finite element model of GFRP dowelled mortise and tenon joint using Kempas species," *AIP Conference Proceedings* 3026(1), article 080018. DOI: 10.1063/5.0200914

De Queiroz, K. (2006). "The PhyloCode and the distinction between taxonomy and nomenclature," *Systematic Biology*, (P. Lewis, ed.), 55(1), 160-162. DOI: 10.1080/10635150500431221

Demirci, S., Diler, H., Kasal, A., and Erdil, Y. Z. (2020). "Bending moment resistances of L-shaped furniture frame joints under tension and compression loadings," *Wood Research* 65(6), 975-988. DOI: 10.37763/wr.1336-4561/65.6.975988

Ecke, G. (1986). *Chinese Domestic Furniture in Photographs and Measured Drawings*. Courier Corporation.

Eckelman, C. A., and Haviarova, E. (2011). "Rectangular mortise and full-width tenon joints in ready-to-assemble light-frame timber constructions," *Wood and Fiber Science* 43(4), 346-352.

Elek, L., Kovacs, Z., Csoka, L., and Agarwal, C. (2020). "Evaluation of the effect of optimal fit criteria on the compressive strength of open mortise and tenon corner joints," *European Journal of Wood and Wood Products* 78(2), 351-363. DOI: 10.1007/s00107-020-01509-w

Feio, A. O., Lourenço, P. B., and Machado, J. S. (2014). "Testing and modeling of a traditional timber mortise and tenon joint," *Materials and Structures* 47(1–2), 213-225. DOI: 10.1617/s11527-013-0056-y

Fischer, C., and Gregor, S. (2011). "Forms of reasoning in the design science research process," in: *Service-Oriented Perspectives in Design Science Research*, Lecture Notes in Computer Science, H. Jain, A. P. Sinha, and P. Vitharana (eds.), Springer Berlin Heidelberg, Berlin, Heidelberg, 17-31. DOI: 10.1007/978-3-642-20633-7_2

Guan, H. (2007). "Modern furniture structures. 3rd Chapter: Traditional wooden furniture structure and lts modernization (in Chinese)," *Furniture* (3), 48-53. DOI: DOI: 10.16610/j.cnki.jiaju.2007.03.004

Hassan, R., Ibrahim, A., and Ahmad, Z. (2023). "Structural behaviour of mortise and tenon joints," in: *Timber Connections: Mortise and Tenon Structural Design*, R. Hassan, A. Ibrahim, and Z. Ahmad (eds.), Springer Nature, Singapore, pp. 25-42. DOI: 10.1007/978-981-19-2697-6_3

He, J., Yu, P., Wang, J., Yang, Q., Han, M., and Xie, L. (2021). "Theoretical model of bending moment for the penetrated mortise-tenon joint involving gaps in traditional timber structure," *J. Building Engineering* 42. DOI: 10.1016/j.jobe.2021.103102

Hu, W., and Chen, B. (2021). "A methodology for optimizing tenon geometry dimensions of mortise-and-tenon joint wood products," *Forests* 12(4). DOI: 10.3390/f12040478

Hu, W., and Guan, H. (2019). "A finite element model of semi-rigid mortise-and-tenon joint considering glue line and friction coefficient," *Journal of Wood Science* 65(1), article 14. DOI: 10.1186/s10086-019-1794-4

Hu, W., and Liu, N. (2020). "Comparisons of finite element models used to predict bending strength of mortise-and-tenon joints," *BioResources* 15(3), 5801-5811. DOI: 10.15376/biores.15.3.5801-5811

Huang, Z., Bai, H., Ma, S., Zhang, J., Chen, Y., and Li, H. (2023). "Large-scale testing of the mortise and tenon joint performance of the tunnel lining of prefabricated frame tunnels," *Tunnelling and Underground Space Technology* 131, article 104828. DOI: 10.1016/j.tust.2022.104828

Iraola, B., Cabrero, J. M., Basterrechea-Arévalo, M., and Gracia, J. (2021). "A geometrically defined stiffness contact for finite element models of wood joints," *Engineering Structures* 235, article 112062. DOI: 10.1016/j.engstruct.2021.112062

Kasal, A., Smardzewski, J., Kuşkun, T., and Erdil, Y. Z. (2016). "Numerical analyses of various sizes of mortise and tenon furniture joints," *BioResources* 11(3), 6836-6853. DOI: 10.15376/biores.11.3.6836-6853

Kaygin, B., Yorur, H., and Uysal, B. (2016). "Simulating strength behaviors of corner joints of wood constructions by using finite element method," *Drvna Industrija* 67(2), 133-140. DOI: 10.5552/drind.2016.1503

Kundisch, D., Muntermann, J., Oberländer, A. M., Rau, D., Röglinger, M., Schoormann, T., and Szopinski, D. (2022). "An update for taxonomy designers: Methodological guidance from information systems research," *Business & Information Systems*

Engineering 64(4), 421-439. DOI: 10.1007/s12599-021-00723-x
Li, X., Zhao, J., Ma, G., and Huang, S. (2015). "Experimental study on the traditional timber mortise-tenon joints," *Advances in Structural Engineering* 18(12), 2089-2102. DOI: 10.1260/1369-4332.18.12.2089
Li, Z. (2015). *Traditional Woodworking Tools in Chinese Architecture (in Chinese)*, Tongji University Press, Shanghai, China.
Li, Z., Lin, K., Fang, H., Yu, H., Wang, J., Miao, Y., Wang, L., Li, J., and Jiang, W. (2023). "The mortise and tenon structure enabling lamellar carbon composites of ultra-high bending strength," *Journal of Materials Science & Technology* 133, 249-258. DOI: 10.1016/j.jmst.2022.03.030
Liang, M., Liu, Y., and Geng, X. (2021). "Research on the innovative application of Chinese traditional mortise and tenon joint in modern furniture (in Chinese)," *Furniture & Interior Design* (11), 14-17.
Liu, T., and Lin, M. (2020). "Research overview on traditional furniture under the digital technology (in Chinese)," *Design* 33(13), 5.
Ma, L., Xue, J., Dai, W., Zhang, X., and Zhao, X. (2020). "Moment-rotation relationship of mortise-through-tenon connections in historic timber structures," *Construction and Building Materials* 232. DOI: 10.1016/j.conbuildmat.2019.117285
Nickerson, R. C., Varshney, U., and Muntermann, J. (2013). "A method for taxonomy development and its application in information systems," *European Journal of Information Systems* 22(3), 336-359. DOI: 10.1057/ejis.2012.26
Ohmori, K., and Kunii, T. L. (2011). "Visualized deformation of joint to understand jointing process by homotopy theory and attaching maps," in: *2011 Int. Conf. on Cyberworlds*, IEEE, Calgary, AB, Canada, pp. 203-210. DOI: 10.1109/CW.2011.14
Pan, Y., An, R., You, W., and Fan, Y. (2024). "A mechanical model used for the multifactor analysis of through-tenon joints in traditional Chinese timber structures," *Int. J. Architectural Heritage* 18(4), 551-576. DOI: 10.1080/15583058.2023.2173106
Qiao, W., Wang, Z., Wang, D., and Zhang, L. (2022). "A new mortise and tenon timber structure and its automatic construction system," *Journal of Building Engineering* 44. DOI: 10.1016/j.jobe.2021.103369
Rogowski, G. (2002). *The Complete Illustrated Guide to Joint*, The Taunton Press.
Shang, B., Chen, Z., Ma, Q., and Tan, Y. (2023). "A comprehensive mortise and tenon structure selection method based on Pugh's controlled convergence and rough Z-number MABAC method," *PLOS ONE* 18(5), article e0283704. DOI: 10.1371/journal.pone.0283704
Smardzewski, J. (2015). *Furniture Design*. Springer International Publishing. DOI: 10.1007/978-3-319-19533-9
Sun, Q. (2021). "Structure, paradigms, and symbols: Aesthetic shifts in traditional mortise and tenon structure (in Chinese)," *Journal of Hebei University of Science and Technology (Social Sciences Edition)* 21(1), 37-43, article 97. DOI: 10.7535/j.issn.1671-1653.2021.01.006
Švajlenka, J., and Kozlovská, M. (2020). "Evaluation of the efficiency and sustainability of timber-based construction," *Journal of Cleaner Production* 259, article 120835. DOI: 10.1016/j.jclepro.2020.120835
Taghiyari, H. R., Noori, H., and Eckelman, C. A. (2018). Effect of end connections on mid-span load capacity of laminated particleboard bookshelves. *Wood Material Science & Engineering* 13(4), 231-235. DOI: 10.1080/17480272.2017.1356866
Tankut, N., Tankut, A. N., and Zor, M. (2014). "Finite element analysis of wood

materials," *Drvna industrija* 65(2), 159-171. DOI: 10.5552/drind.2014.1254
Tsai, H.-C., Lee, A.-S., Lee, H.-N., and Hooper, H. H. (Buddy). (2022). "Use of similarity of triangular fuzzy numbers and a derivation calculation formula in assessment of mortise-tenon joints applied in the joint category of regional Taiwan skills competitions," *Sustainability* 14(14), article 8608. DOI: 10.3390/su14148608
Uysal, M., Haviarova, E., and Eckelman, C. A. (2015). "A comparison of the cyclic durability, ease of disassembly, repair, and reuse of parts of wooden chair frames," *Materials & Design* 87, 75-81. DOI: 10.1016/j.matdes.2015.08.009
Van Nimwegen, S. E., and Latteur, P. (2023). "A state-of-the-art review of carpentry connections: From traditional designs to emerging trends in wood-wood structural joints," *J. Building Engineering* 78, article 107089. DOI: 10.1016/j.jobe.2023.107089
Wu, B., and Geng, X. (2015). "Exploring innovative design based on the constructivist idea of mortise and tenon structure (in Chinese)," *Furniture* (4), article 5. DOI: CNKI:SUN:JIJU.0.2015-04-014
Wu, C., Xue, J., Zhou, S., and Zhang, F. (2021a). "Seismic performance evaluation for a traditional Chinese timber-frame structure," *International Journal of Architectural Heritage* 15(12), 1842-1856. DOI: 10.1080/15583058.2020.1731626
Wu, W., Zhu, J., Xu, W., Han, F., Wu, X., and Wang, X. (2021b). "Innovative design of modern mortise and tenon structure under the concept of green reduction," *BioResources* 16(4), 8445-8456. DOI: 10.15376/biores.16.4.Wu
Xie, Q., Zhang, B., Zhang, L., Guo, T., and Wu, Y. (2021). "Normal contact performance of mortise and tenon joint: Theoretical analysis and numerical simulation," *Journal of Wood Science* 67(1). DOI: 10.1186/s10086-021-01963-x
Xue, J., Song, D., and Wu, C. (2021). "Precise finite element analysis of full-scale straight-tenon joints in ancient timber buildings," *International Journal of Architectural Heritage*. DOI: 10.1080/15583058.2021.2017073
Yang, A., and Wang, Q. (2013). "Tenon and mortise arts of Ming Dynasty furniture from form perspective (in Chinese)," *Art Design* (7), 141-142. DOI: 10.16272/j.cnki.cn11-1392/j.2013.07.017
Yilmaz, K., and Burdurlu, E. (2023). "Selection of wooden furniture joints with multi-criteria decision-making techniques," *Wood Material Science & Engineering* 19(2), 311-326. DOI: 10.1080/17480272.2023.2242329
Yue, X., Xiong, X., Xu, X., and Zhang, M. (2024). "Big data for furniture intelligent manufacturing: Conceptual framework, technologies, applications, and challenges," *Int. J. Advanced Manufacturing Technology*. DOI: 10.1007/s00170-024-13719-0
Zhang, B., Xie, Q., Li, S., Zhang, L., and Xue, J. (2023). "Numerical analysis of traditional Chinese timber structure: Simplified finite element model and composite elements of joints," *Journal of Building Engineering* 67, article 106027. DOI: 10.1016/j.jobe.2023.106027
Zhang, L., and Yang, X. (2018). "Discussion on wood structure mortise and tenon technology (in Chinese)," *New Arts* 39(11), 6.
Zhang, T., and Hu, W. (2021). "Numerical study on effects of tenon sizes on withdrawal load capacity of mortise and tenon joint," *Wood Research* 66(2), 321-330. DOI: 10.37763/wr.1336-4561/66.2.321330

Article submitted: April 16, 2024; Peer review completed: May 18, 2024; Revised version received and accepted: June 1, 2024; Published: June 5, 2024.
DOI: 10.15376/biores.19.3.4918-4940